JACS
JOURNAL OF THE AMERICAN CHEMICAL SOCIETY

Communication

pubs.acs.org/JACS

Cellulose Nanocrystals as Chiral Inducers: Enantioselective Catalysis and Transmission Electron Microscopy 3D Characterization

Madhu Kaushik,[†] Kaustuv Basu,[‡] Charles Benoit,[†] Ciprian M. Cirtiu,[†,∥] Hojatollah Vali,[‡,§] and Audrey Moores*[,†]

[†]Centre for Green Chemistry and Catalysis, Department of Chemistry, McGill University, 801 Sherbrooke Street West, Montréal, QC H3A 0B8, Canada

[∥]Direction santé environnement et toxicologie, Institut National de Santé Publique du Québec, 945, avenue Wolfe, 4e étage Sainte-Foy, Quebec, QC G1V 5B3, Canada

[‡]Facility for Electron Microscopy Research, McGill University, 3640 University Street, Montréal, QC H3A 0C7, Canada

[§]Anatomy and Cell Biology, McGill University, 3640 University Street, Montréal, QC H3A 0C7, Canada

Supporting Information

ABSTRACT: Cellulose nanocrystals (CNCs), derived from cellulose, provide us with an opportunity to devise more sustainable solutions to current technological challenges. Enantioselective catalysis, especially heterogeneous, is the preferred method for the synthesis of pure chiral molecules in the fine chemical industries. Cellulose has been long sought as a chiral inducer in enantioselective catalysis. We report herein an unprecedentedly high enantiomeric excess (ee) for Pd patches deposited onto CNCs used as catalysts for the hydrogenation of prochiral ketones in water at room temperature and 4 bar H_2. Our system, where CNCs acted as support and sole chiral source, achieved an ee of 65% with 100% conversions. Cryo-electron microscopy, high-resolution transmission electron microscopy, and tomography were used for the first time to study the 3D structure of a metal functionalized CNC hybrid. It established the presence of sub-nanometer-thick Pd patches at the surface of CNCs and provided insight into the chiral induction mechanism.

Biomaterials are being intensely researched as replacements for existing, nonsustainable systems used in fields such as optics, electronics, environmental science, and catalysis.[1] Modern bioresources blend applicability with sustainability-linked properties including nontoxicity, earth abundance, and biodegradability. Among them, cellulose nanocrystals (CNCs) constitute an exciting example, featuring applications in the polymer and paper industries[2] and as supercapacitors,[3] pH-responsive reversible flocculants,[4] hydrogels,[5] aerogels,[6] and chiral materials.[7] They are readily available from cellulose of both vegetal and bacterial origin, through strong acid hydrolysis or mechanical defibrillation.[8] CNCs' exciting properties arise from their well-defined size and morphology, high specific surface area, high aspect ratio, high crystalline order and chirality, superior mechanical strength, and controllable surface chemistry.[1a,2b,9] Each CNC is a high-aspect-ratio nanocrystal of a homopolymer, with a dimer of glucose, known as cellobiose, as the repeat unit (Figure 1a). Recently, a deeper understanding of this nanomaterial was made possible via transmission electron microscopy (TEM)-based tomography.[10]

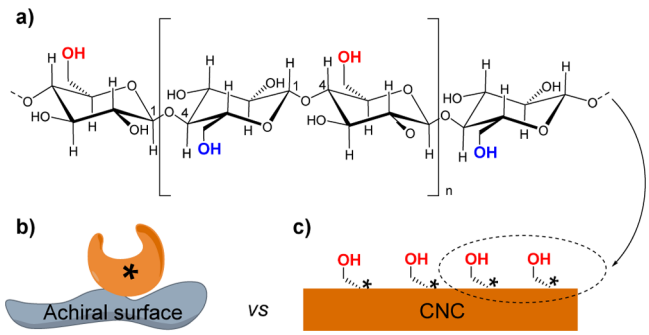

Figure 1. (a) Molecular structure of cellulose nanocrystals (CNCs). (b) Scheme of a 3D chiral molecule-modified surface. (c) Scheme of the 2D surface of a CNC featuring hydroxyl groups oriented in a chiral fashion.

Enantioselective catalysis has been the method of choice to synthesize pure chiral molecules in the pharmaceutical and agrochemical industry.[11] This is largely achieved using homogeneous catalysis, notably organocatalysis.[12] The "chiral pool", provided by nature, is a classical resource for chiral induction.[13] For industrial applications, however, developing heterogeneous versions of enantioselective catalysts is essential[11] because of the importance of their easy separation and recycling in this context,[14] and nanoscience has been an important contributor to creativity in this area.[15]

A typical, and very successful, strategy to induce chirality relied on the use of 3D chiral molecules supported onto 2D material acting as spectators (Figure 1b).[16] The alteration of metal surfaces with strongly interacting chiral modifiers also afforded powerful catalysts.[17] In all these cases, enantioselectivity originated from a three-dimensional, chiral molecular arrangement. The ability to use a 2D chiral structure, especially biobased, to afford enantioselectivity has remained a challenge until today, because the flat nature of such structures typically limited their

Received: February 26, 2015
Published: April 27, 2015

ACS Publications © 2015 American Chemical Society

DOI: 10.1021/jacs.5b02034
J. Am. Chem. Soc. 2015, 137, 6124−6127

ability to interact effectively with incoming substrates (Figure 1c). In the literature, such 2D chiral materials of natural origin, including quartz, silk fibroin, and cellulose,[18] were used as supports for metal or metal oxide catalysts yielding very poor enantioselectivities. The best-known example of this route was reported in the 1950s as a silk-supported Pd catalyst affording a 25% enantiomeric excess (ee) in the hydrogenation of benzylidene oxazolidone.[18a] Harada and Yoshida used modified cellulose−palladium catalyst for asymmetric hydrogenations, where they could not obtain ee above 10% and the results were irreproducible.[18d,19]

While amorphous chiral polymers have a limited ability to be used directly as chiral inducers, highly crystalline and well-defined CNCs have demonstrated interesting chiral properties, mostly exploited in the framework of material science. CNCs in concentrated aqueous suspensions adopt a chiral nematic ordered phase. The formation of this anisotropic phase is interesting as the molecules in these suspensions possess no structural chirality. This property was exploited for producing iridescent films,[20] chiral mesoporous silica[7c] and carbon,[7d] chiral plasmonic films by gold nanorods,[7a] and chirality-specific hydrolysis of amino acid substrates.[7b] In the field of catalysis, CNCs were used as supports for Pd and Au nanoparticles (NPs).[21] Pd NPs deposited onto CNCs were used for hydrogenation and heck coupling reactions by us and others,[22] while the Au counterparts showed activity toward 4-nitrophenol reduction.[23] Ag NPs were also deposited onto CNC and demonstrated antibacterial activity.[24] CNC composites, however, had so far never been applied in enantioselective catalysis. Herein, we show that CNCs could be successfully used as 2D chiral inducers and report an unprecedented 65% ee for the hydrogenation of a prochiral ketone using palladium patches deposited onto CNCs (PdPs@CNCs) in water. We also used TEM tomography to establish the structure of the catalyst and provide insight into the potential chiral induction mechanism.

In order to test the ability of CNC to serve as an enantioselective support, we deposited Pd(0) at the surface of CNCs, following a procedure developed by our group.[22a] CNCs, in freeze-dried form, were resuspended in water and exposed to an aqueous acidic $PdCl_2$ solution (Scheme 1). $PdCl_2$ could

Scheme 1. Synthesis of the Catalyst PdPs@CNCs via Hydrogenation of an Aqueous Mixture of a CNC Suspension and a $PdCl_2$ Solution

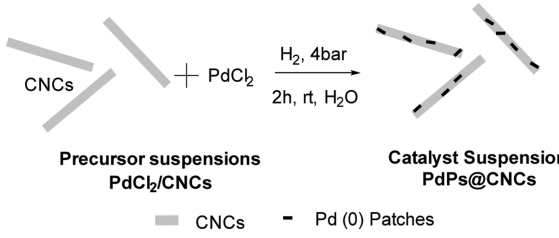

interact with both hydroxyl groups at the CNC surface as well as the sulfate ester groups introduced during CNC extraction from cellulose. The solution was then exposed to mild H_2 pressure, causing Pd reduction and deposition onto the CNC surface, yielding PdPs@CNCs.[22a] The resulting hybrid material was active for the hydrogenation of phenol and the Heck reaction. For the present work, we turned to hydrogenation of prochiral ketones. The reaction proceeded well under mild conditions, using 4 bar of hydrogen at room temperature in water. Under these conditions, acetophenone (**1**) was 100% converted in 2 h, with a yield of 87% for 1-phenylethanol (Scheme 2).

Scheme 2. Enantioselective Ketone Hydrogenation Using PdPs@CNCs as Catalyst

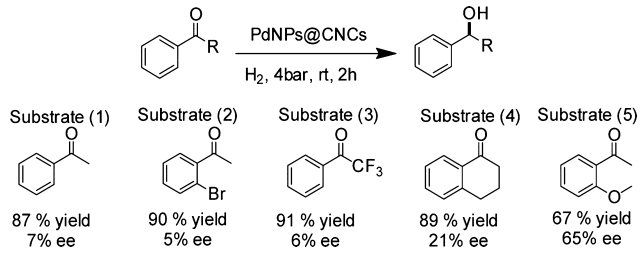

Interestingly, an ee of 7% was measured. Although very low, this ee demonstrated that the CNC surface had some chiral induction activity, as it was the only chiral source present. We selected 4 more ketones with different substitution schemes and steric bulk, in hope of achieving more exciting ees.

2−**5** also gave 100% conversions and excellent yields. **2** and **3**, like **1**, gave low ee between 5% and 7%. Hydrogenation of the bulkier substrate **4**, gave an increased ee of 21%. Interestingly, **5**, with an additional ether functionality susceptible to H-bond with the CNC surface, afforded a high 65% ee, an unprecedented ee for 2D chiral induction.

To evaluate the stability of this catalyst, recycling tests were performed and demonstrated that the aqueous suspension of PdPs@CNCs could be reused by simple phase separation up to three times with no loss of activity and enantioselectivity. The fourth and fifth cycles did lead to a drop in activity, but the enantioselectivity was preserved (Supporting Information (SI), Figure S1). Besides, no conversion was measured when using unmodified CNCs or unsupported Pd NPs, which tended to grow and form palladium black (SI, Table S1). To determine whether the catalysis was truly heterogeneous, a poisoning experiment using CS_2 was also performed. The addition of 0.5 equiv of CS_2 to the reaction mixture made the catalyst totally ineffective under the reaction conditions used.[25] These results confirmed that (i) the reaction of hydrogenation happened heterogeneously and palladium metal was the active catalyst, and (ii) CNCs were not just a mere support to the Pd catalyst but participated actively in the reaction. The CNC surface is lined with hydroxymethyl groups at the sugar cycle C6 position (Figure 1). These primary hydroxyl groups are pointing outward in an organized, periodic, and chiral fashion, assigning a level of molecular preorganization to the CNC surface (Figure 1a,c). Remarkably, in this system, only CNCs possessed the chirality necessary to explain the ee obtained, as large as 65% with substrate **5**. It is interesting to note as well that bulk around the hydrogenated C═O double bond was critical and justified an ee enhancement from 7% to 25%, between substrates **1** and **4**. The results also suggested that an increased interaction of the substrate with the CNC surface resulted in an increased ee. Substrate **5** possessed an additional ether functionality susceptible to improve interaction with polar surfaces such as CNC, but also with metal surfaces.[26] A complete morphological characterization of the catalyst was performed to gain further insight into the potential chiral induction mechanism.

The catalyst was thus imaged by TEM without heavy metal staining. Imaging in cryo-TEM was carried out to investigate the structure of the composite nanomaterial PdPs@CNCs under conditions as close to native as possible. In 2014, cryo-TEM and

DOI: 10.1021/jacs.5b02034
J. Am. Chem. Soc. 2015, 137, 6124−6127

tomography were already used by Ikkala and coll. to obtain the 3D structure of unmodified CNC.[8] In the present work, a thin vitrified layer of an aqueous suspension of PdPs@CNCs was imaged in a cryo-TEM with a direct detection device (DDD) at an accelerating voltage of 300 kV. In order to have a comparison stand point, we also analyzed under the same conditions a CNC suspension exposed to $PdCl_2$, without H_2 reduction ($PdCl_2$/CNCs). Although $PdCl_2$/CNCs is the precursor to PdPs@CNCs, it is not active for hydrogenation catalysis.[19a] Cryo-TEM images of both samples are presented in Figures 2 and S2−S12,

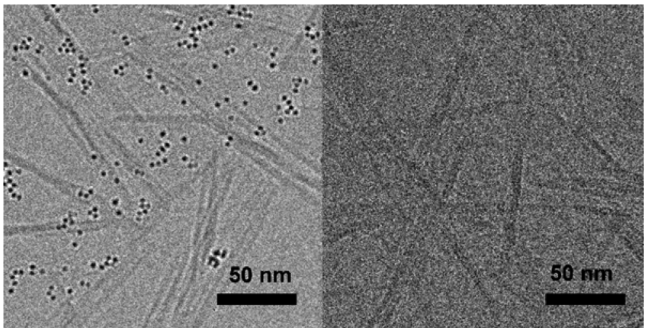

Figure 2. Cryo-TEM images of $PdCl_2$/CNCs (left) and PdPs@CNCs (right).

and all show well dispersed and well-defined CNC whiskers of 150−200 nm in length and 4−6 nm in width, which is in agreement with values reported in the literature.[2b] Surprisingly, no Pd NPs could be seen at this resolution for PdPs@CNCs suspensions, the active catalyst in this study. A tilt series from −60° to +60° was acquired on PdPs@CNCs and its 3D structure was analyzed from the reconstructed tomograms (Figures 3 and

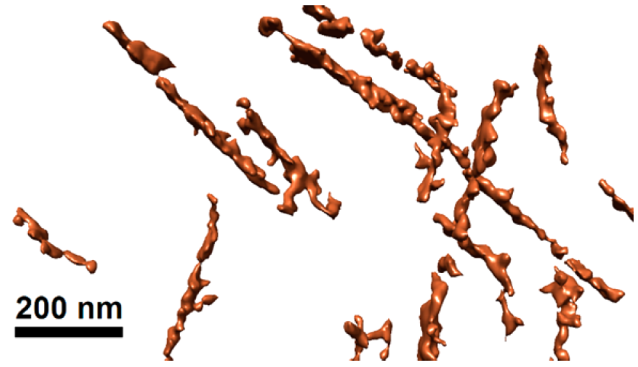

Figure 3. TEM tomogram of PdPs@CNCs in cryo conditions.

S13−S16, and SI movies S1 and S2). In both tomograms and movies, CNC whiskers can be seen as individual rods, consistent with the observations of Ikkala and coll.[8] On the other hand, for the $PdCl_2$/CNCs sample, well-defined, high-contrast NPs of 2.7 ± 0.4 nm in diameter were observed. These particles did not appear to be correlated to the presence of CNCs. The reconstructed tomograms of $PdCl_2$/CNC (Figures S17 and S18, and movies S3 and S4) showed that these particles were segregated at the surface of the vitrified ice layer, and could be caused by $PdCl_2$ precipitation.

To complement these findings, both samples were air-dried on Cu TEM grids and imaged at room temperature using a DDD and a phase plate at 300 kV, enabling higher resolution images in comparison to the images collected in cryo-TEM. Interestingly, NPs were observed in both samples, but in far greater amounts for the precursor, $PdCl_2$/CNCs. More importantly, on PdPs@CNCs sample grids, patches of Pd were seen on the surfaces of the CNCs (Figures 4 and S19−S22). These patches appeared as

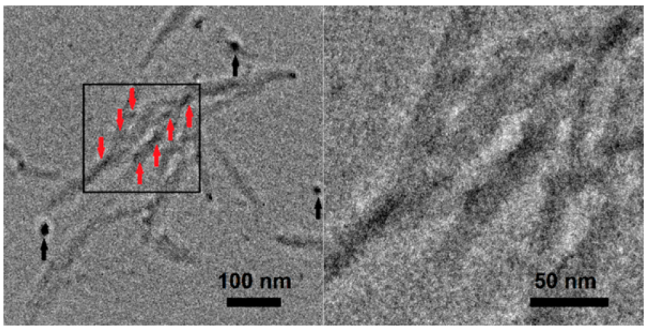

Figure 4. TEM images of PdPs@CNCs recorded using a DDD. On the left, few isolated CNCs featuring plates (red arrows) on their surface. Larger NPs (black arrows) are very few and not physically linked to CNC. On the right, a close up view of the area indicated by the box on the left and revealing Pd patches.

parallelepipeds of 2−5 nm in width and 5−20 nm in length (Figure 4, right). Their very low contrast suggest that they are possibly only a few atoms in depth. The quality of the images obtained in terms of contrast for both the metal and the organic phase simultaneous was remarkable. Energy-dispersive spectroscopy (EDS) was carried out on both samples, and revealed the presence of Pd in PdPs@CNCs and Pd and Cl in $PdCl_2$/CNCs (Figures S24 and S25). These results suggest the active catalyst, PdPs@CNCs, was composed of CNC and Pd(0) originated from the reduction of $PdCl_2$, as established from EDS and the catalytic activity. This metal was present as sub-nanometer-thick patches deposited on CNC as observed in high resolution TEM, but too thin to be observed in cryo-TEM.

In the TEM images obtained from the air-dried sample of PdPs@CNCs, a few Pd(0) NPs of sizes ∼2−5 nm were observed. Their absence in cryo-TEM demonstrates that these were artifacts arising from the drying process. In past accounts, including from our group,[19a] these were incorrectly thought to be responsible for catalysis. In this work, the comparison of cryo-TEM, which prevents drying-driven aggregation and better preserves the near-native state of the suspension during catalysis, with air-dried imaging using DDD and phase plate technologies uniquely informs the true nature of PdPs@CNCs as a catalytic material.

Subtle energy differences on the surface of the catalyst has been demonstrated to result in efficient stereodirection.[17a] The chiral arrangement of H-bonding groups on the CNC surface is likely to be responsible for the prochiral substrates differentiation and thus the high ee observed. On one end, the molecular preorganization of hydroxyl groups at the CNC surface may directly interact with the incoming pro-chiral substrate and orient it along one orientation over the other. In this hypothesis, the ketone reagent could interact simultaneously with the CNC surface, to be preferentially oriented as a function of its prochiral properties, and the Pd patches surface to be successfully hydrogenated. The effect of catalyst support on the mechanism of hydrogenation has been previously reported.[27] Alternatively, as the Pd patches observed were very thin, the CNC could lead to the formation of a chirally active Pd surface, as has been observed previously on Au NPs.[28]

DOI: 10.1021/jacs.5b02034
J. Am. Chem. Soc. 2015, 137, 6124−6127

In this investigation, we have established the role of CNCs in chiral induction in hydrogenation of prochiral ketones. Pd patches are important for activating the hydrogenation reactions, whereas the CNCs brought in the enantioselection. Cryo-TEM and tomography in conjunction with DDD technology demonstrated the direct contact between the Pd patches and their low-density support. Conceptually, these results offer an opportunity to use cellulose, in the form of the highly crystalline CNC, directly in asymmetric catalysis. Our future work will focus on expanding the scope of the reaction and improving enantioselectivity by achiral surface modification of CNCs, and kinetic investigations to establish further reaction mechanism(s).

■ ASSOCIATED CONTENT

Supporting Information

Experimental details and complete TEM data. The Supporting Information is available free of charge on the ACS Publications website at DOI: 10.1021/jacs.5b02034.

■ AUTHOR INFORMATION

Corresponding Author

*audrey.moores@mcgill.ca

Notes

The authors declare no competing financial interest.

■ ACKNOWLEDGMENTS

We thank the Natural Science and Engineering Research Council of Canada (NSERC) Discovery Grant program, the Canada Foundation for Innovation (CFI), the Canada Research Chairs (CRC), the Fonds de Recherche du Québec—Nature et Technologies (FRQNT) Equipe program, the Centre for Green Chemistry and Catalysis (CGCC), NSERC-Collaborative Research and Training Experience (CREATE) in Green Chemistry, and McGill University for their financial support. We thank FP Innovations for providing the CNCs, and Dr. S. Kelly Sears and Dr. David Liu for their technical help and discussions on TEM.

■ REFERENCES

(1) (a) Habibi, Y.; Lucia, L. A.; Rojas, O. J. *Chem. Rev.* **2010**, *110*, 3479. (b) Thakur, V. K.; Thakur, M. K.; Raghavan, P.; Kessler, M. R. *ACS Sust. Chem. Eng.* **2014**, *2*, 1072. (c) Rak, M. J.; Friscic, T.; Moores, A. *Faraday Discuss.* **2014**, *170*, 155.

(2) (a) Moon, R. J.; Martini, A.; Nairn, J.; Simonsen, J.; Youngblood, J. *Chem. Soc. Rev.* **2011**, *40*, 3941. (b) Klemm, D.; Kramer, F.; Moritz, S.; Lindström, T.; Ankerfors, M.; Gray, D.; Dorris, A. *Angew. Chem., Int. Ed.* **2011**, *50*, 5438. (c) Ramires, E. C.; Dufresne, A. *Tappi J.* **2011**, *10*, 9. (d) BelHaaj, S.; Ben Mabrouk, A.; Thielemans, W.; Boufi, S. *Soft Matter* **2013**, *9*, 1975.

(3) (a) Liew, S. Y.; Thielemans, W.; Walsh, D. A. *J. Phys. Chem. C* **2010**, *114*, 17926. (b) Liew, S. Y.; Walsh, D. A.; Thielemans, W. *RSC Adv.* **2013**, *3*, 9158.

(4) Kan, K. H. M.; Li, J.; Wijesekera, K.; Cranston, E. D. *Biomacromolecules* **2013**, *14*, 3130.

(5) Yang, J.; Han, C.-R.; Duan, J.-F.; Ma, M.-G.; Zhang, X.-M.; Xu, F.; Sun, R.-C.; Xie, X.-M. *J. Mater. Chem.* **2012**, *22*, 22467.

(6) Yang, X.; Cranston, E. D. *Chem. Mater.* **2014**, *26*, 6016.

(7) (a) Querejeta-Fernández, A.; Chauve, G.; Methot, M.; Bouchard, J.; Kumacheva, E. *J. Am. Chem. Soc.* **2014**, *136*, 4788. (b) Serizawa, T.; Sawada, T.; Wada, M. *Chem. Commun.* **2013**, *49*, 8827. (c) Shopsowitz, K. E.; Qi, H.; Hamad, W. Y.; MacLachlan, M. J. *Nature* **2010**, *468*, 422. (d) Shopsowitz, K. E.; Hamad, W. Y.; MacLachlan, M. J. *J. Am. Chem. Soc.* **2011**, *134*, 867. (e) Qi, H.; Shopsowitz, K. E.; Hamad, W. Y.; MacLachlan, M. J. *J. Am. Chem. Soc.* **2011**, *133*, 3728. (f) Giese, M.; Blusch, L. K.; Khan, M. K.; MacLachlan, M. J. *Angew. Chem., Int. Ed.* **2015**, *54*, 2888. (g) Khan, M. K.; Bsoul, A.; Walus, K.; Hamad, W. Y.; MacLachlan, M. J. *Angew. Chem.* **2015**, *127*, 4378.

(8) Holt, B. L.; Stoyanov, S. D.; Pelan, E.; Paunov, V. N. *J. Mater. Chem.* **2010**, *20*, 10058.

(9) Lin, N.; Huang, J.; Dufresne, A. *Nanoscale* **2012**, *4*, 3274.

(10) Majoinen, J.; Haataja, J. S.; Appelhans, D.; Lederer, A.; Olszewska, A.; Seitsonen, J.; Aseyev, V.; Kontturi, E.; Rosilo, H.; Österberg, M.; Houbenov, N.; Ikkala, O. *J. Am. Chem. Soc.* **2013**, *136*, 866.

(11) Ding, K.; Uozumi, Y. *Handbook of asymmetric heterogeneous catalysis*; Wiley VCH: Weinheim, 2008.

(12) Dalko, P. I. *Enantioselective organocatalysis*; Wiley VCH: Weinheim, 2007.

(13) Katsuki, T.; Sharpless, K. B. *J. Am. Chem. Soc.* **1980**, *102*, 5974.

(14) (a) Cole-Hamilton, D. J. *Science* **2003**, *299*, 1702. (b) *Catalyst separation, recovery and recycling: chemistry and process design*; Cole-Hamilton, D. J., Tooze, R. P., Eds.; Springer: The Netherlands, 2006; Vol. *30*. (c) Pélisson, C.-H.; Denicourt-Nowicki, A.; Meriadec, C.; Greneche, J.-M.; Roucoux, A. *ChemCatChem* **2014**, *7*, 309.

(15) (a) Astruc, D.; Lu, F.; Aranzaes, J. R. *Angew. Chem., Int. Ed.* **2005**, *44*, 7852. (b) Polshettiwar, V.; Varma, R. S. *Green Chem.* **2010**, *12*, 743. (c) Polshettiwar, V.; Luque, R.; Fihri, A.; Zhu, H.; Bouhrara, M.; Basset, J.-M. *Chem. Rev.* **2011**, *111*, 3036. (d) Wang, D.; Astruc, D. *Chem. Rev.* **2014**, *114*, 6949. (e) Astruc, D. *Nanoparticles and Catalysis*; Wiley-VCH: Weinheim, 2008.

(16) (a) Song, C. E.; Sang-gi, L. *Chem. Rev.* **2002**, *102*, 3495−3524. (b) Baiker, A. *J. Mol. Catal. A: Chem.* **1997**, *115*, 473. (c) Heitbaum, M.; Glorius, F.; Escher, I. *Angew. Chem., Int. Ed.* **2006**, *45*, 4732.

(17) (a) Demers-Carpentier, V.; Goubert, G.; Masini, F.; Lafleur-Lambert, R.; Dong, Y.; Lavoie, S.; Mahieu, G.; Boukouvalas, J.; Gao, H. L.; Rasmussen, A. M. H.; Ferrighi, L.; Pan, Y. X.; Hammer, B.; McBreen, P. H. *Science* **2011**, *334*, 776. (b) Kyriakou, G.; Beaumont, S. K.; Lambert, R. M. *Langmuir* **2011**, *27*, 9687.

(18) (a) Akabori, S.; Sakurai, S.; Izumi, Y.; Fujii, Y. *Nature* **1956**, *178*, 323. (b) Beamer, R. L.; Fickling, C. S.; Ewing, J. H. *J. Pharm. Sci.* **1967**, *56*, 1029. (c) Schwab, G.-M.; Rudolph, L. *Naturwissenschaften* **1932**, *20*, 363. (d) Harada, K.; Yoshida, T. *Naturwissenschaften* **1970**, *57*, 131.

(19) Mallat, T.; E, O.; A, B. *Chem. Rev.* **2007**, *107*, 4863.

(20) (a) Revol, J.-F.; Godbout, L.; Dong, X.-M.; Gray, D. G.; Chanzy, H.; Maret, G. *Liq. Cryst.* **1994**, *16*, 127. (b) Picard, G.; Simon, D.; Kadiri, Y.; LeBreux, J.; Ghozayel, F. *Langmuir* **2012**, *28*, 14799. (c) Cranston, E. D.; Gray, D. G. *Biomacromolecules* **2006**, *7*, 2522.

(21) Lam, E.; Male, K. B.; Chong, J. H.; Leung, A. C. W.; Luong, J. H. T. *Trends Biotechnol.* **2012**, *30*, 283.

(22) (a) Cirtiu, C. M.; Dunlop-Brière, A. F.; Moores, A. *Green Chem.* **2011**, *13*, 288. (b) Rezayat, M.; Blundell, R. K.; Camp, J. E.; Walsh, D. A.; Thielemans, W. *ACS Sust. Chem. Eng.* **2014**, *2*, 1241. (c) Zhou, P.; Wang, H.; Yang, J.; Tang, J.; Sun, D.; Tang, W. *Ind. Eng. Chem. Res.* **2012**, *51*, 5743. (d) Wu, X.; Lu, C.; Zhang, W.; Yuan, G.; Xiong, R.; Zhang, X. *J. Mater. Chem. A* **2013**, *1*, 8645.

(23) Lam, E.; Hrapovic, S.; Majid, E.; Chong, J. H.; Luong, J. H. T. *Nanoscale* **2012**, *4*, 997.

(24) Xiong, R.; Lu, C.; Zhang, W.; Zhou, Z.; Zhang, X. *Carbohydr. Polym.* **2013**, *95*, 214.

(25) Luska, K. L.; Moores, A. *Adv. Synth. Catal.* **2011**, *353*, 3167.

(26) Hou, Z.; Theyssen, N.; Brinkmann, A.; Leitner, W. *Angew. Chem.* **2005**, *117*, 1370.

(27) Cirtiu, C. M.; Hassani, H. O.; Bouchard, N.-A.; Rowntree, P. A.; Ménard, H. *Langmuir* **2006**, *22*, 6414.

(28) Andreiadis, E. S.; Vitale, M. R.; Mézailles, N.; Le Goff, X.; Le Floch, P.; Toullec, P. Y.; Michelet, V. *Dalton Trans.* **2010**, *39*, 10608.

DOI: 10.1021/jacs.5b02034
J. Am. Chem. Soc. 2015, 137, 6124−6127